Experiments in Fluids 22 (1997) 463–472 © Springer-Verlag 1997

The impact of a single drop on a wetted solid surface

G. E. Cossali, A. Coghe, M. Marengo

Abstract The impact of single drops on a thin liquid film was studied to understand the mechanism of secondary atomisation of sprays colliding on a wetted, cold, solid surface. To span a wide range of conditions various mixtures of water and glycerol were used. The use of Weber number, Ohnesorge number and non-dimensional film thickness to describe the peculiarities of the phenomenon allowed to carry out the experiments under appropriate similarity conditions. The impact of millimetric drops was analysed in detail by photographic means, using both still photography to study impact morphology, and laser sheet visualisation to investigate secondary droplet formation. Two mechanisms of splash were identified, depending essentially on the liquid viscosity (Ohnesorge number), a parameter which appears to play an important role also in defining the splash morphology. A photographic documentation is annexed. The characteristic times of the crown formation, the non-linear evolution of cusps (jet formation) and the surface roughness influence are further discussed. The experimental results allow to propose an empirical correlation for the splashing/deposition limit, for a wide range of conditions, and a comparison to available previous works is presented. The influence of the film thickness and liquid viscosity on the splash is confirmed and quantified.

Received: 1 March 1996/Accepted: 12 November 1996

G. E. Cossali
Università di Bergamo,
Via Marconi, 5, I-24044, Dalmine, Bergamo, Italy

A. Coghe, M. Marengo[1]
Politecnico di Milano, P. za Leonardo da Vinci 32,
I-20133 Milano-Italy

Correspondence to: A. Coghe

[1]*Present address*: Lehrstuhl für Strömungsmechanik, Prof. F. Durst, Cauarstr. 4, D-91058 Erlangen, Germany

The experiments were performed at CNPM-CNR laboratories in Milan. The authors would like to thank Mr. Valentino Michelotti and Mr. Stefano Milza for their work during the experiments. Mr Gianni Brunello for his assistance, Ing. Bollina for the surface treatment and roughness measurement of the aluminium disk. We are also indebted to Prof. Cam Tropea and Prof. A.L. Yarin for many helpful and stimulating discussions.

List of Symbols

Bo	Bond number ($=\rho g h^2/\sigma$)
Ca	capillary number ($=\mu V/\sigma$)
D	nozzle diameter
f	impact frequency
f_{nd}	non-dimensional impact frequency ($=f\,\phi/V$)
Fr	Froude number ($=V^2\phi/g$)
h	film thickness
H	crown height
K	$We\,Oh^{-0.4}$
K_L	splashing/deposition limit
N	number of secondary droplets
N_{jet}	number of jets detaching from the crown
Oh	Ohnesorge number ($=\mu/(\phi\sigma\rho)^{1/2}$)
R_a	roughness
$R_{c,nd}$	nondimensional crown radius ($=R_c/\phi$)
R_c	crown radius
Re	Reynolds number ($=\rho V\phi/\mu$)
R_{nd}	non-dimensional roughness ($=R_a/\phi$)
t	time
t_s	splash beginning time
U_g	gravitation potential energy
U_s	surface potential energy
V	terminal drop velocity
We	Weber number ($=\rho V^2\phi/\sigma$)
We_{cr}	critical Weber number
We_d	deposition Weber number
We_s	splash Weber number
Y	splashing/deposition parameter

Greek symbols

α	drop impact angle
δ	non-dimensional film thickness ($=h/\phi$)
ϕ	drop diameter
Φ	coalescence parameter
ϕ_{jet}	jet diameter
λ	viscosity length ($=(\mu/\rho f)^{1/2}\sigma\rho/\mu^2$)
μ	liquid viscosity
ρ	liquid density
σ	surface tension
τ	non-dimensional time ($=t\,\phi/V$)
τ_0	splash time scale ($=\phi/V$)
τ_s	nondimensional splash beginning time ($=t_s/\tau_0$)

1 Introduction

The study of the splashing of drops on a liquid film has a great number of applications. Fields such as the erosion of soil,

atomisation of dangerous liquids, dispersal of spores and microorganisms, atomisation of the fuel after a plane crash, surface cooling by water sprays, are some of those possible where a deeper knowledge of the drop–wall interaction phenomena can be usefully applied. In internal combustion engines, the increased probability for the fuel to impact on intake ducts (gasoline engines) or on piston bowl (direct injection diesel engines), due to some new arrangements of the engine parameters (higher injection pressure, smaller cylinder dimensions), prompted in recent years many investigations on the spray-wall interaction. In many of the papers about spray dynamics modelling, the numerical codes use the results of Wachters and Westerling (1966) to analyse the general impingement of spray drops against a solid surface. Wachters and Westerling (1966) performed an analysis of the splashing regimes and heat transfer for impact of drops, of different liquids and diameter of 2–3 mm, against a hot (about 400°C) dry wall. They used a single dimensionless number (Weber number) to describe the disintegration process of drops after impact. For $We < 30$, no splash was observed; in the range $30 < We < 80$, the drop broke after being bounced back from the plate, and, for $We > 80$, splash occurred. These limits are quite different from those found for a cold wall, and described below, showing that the wall temperature influence on the splash parameters is not negligible, especially for temperatures near to the Leidenfrost temperature. However, when the wall is covered by a liquid layer, the film morphology is expected not to change significantly till temperatures close to the Leidenfrost temperature but an indirect influence comes from the dependence of the liquid characteristics (viscosity, surface tension and density) on temperature; thus the results about splashing on cold wetted surface may be extrapolated to hot wall conditions as far as wall temperature is not close to the Leidenfrost limit and liquid characteristics are evaluated at the proper temperature. Leidenfrost temperature was found to increase with ambient pressure (Emmerson and Snoek 1978), and in Diesel spray, for example, the high chamber pressure at the end of compression makes the wet wall condition after the spray's impact to be the most likely (Naber and Farrel 1993).

The present work reports results obtained for the thin film regime, where the surface roughness was purposely reduced by proper treatment of the impact surface. A review of the available publications on the dynamics of the drop-wall impact is reported in the next section, the third section describes the experimental set-up and analyses the effect of experimental uncertainties on the results, the fourth section reports qualitative and quantitative results on splash morphology and splashing/deposition limit, and a comparison to the available experiments and theoretical predictions. The paper ends with the concluding remarks.

2
The dynamics of drop-wall impact

Although the literature concerning the general drop-wall impact problem is extremely wide (see Rein 1993 for a review), studies of the splashing phenomena on a thin liquid film (where the film thickness is comparable to diameter of impact drop, but is much greater than surface roughness depth) is extremely lacking. The dynamics of the impact of a single liquid drop on a wall covered by a liquid film depend on the dynamic characteristics of the impinging drops (diameter (ϕ), terminal drop velocity (V)), on the physical characteristics of the liquid (viscosity (μ), density (ρ), surface tension (σ)) and on the film thickness (h). The evolution of the liquid film flow field after the impact is driven by the opposing action of surface and inertial forces, and damped by the viscous forces. Also gravity may play a role in a way similar to that of the surface forces.

The Weber number ($We = \rho V^2 \phi / \sigma$), the Ohnesorge number ($Oh = \mu / (\phi \sigma \rho)^{1/2}$), the non-dimensional film thickness ($\delta = h/\phi$), the Bond number ($Bo = \rho g h^2 / \sigma$), the Reynolds number ($Re = \rho V \phi / \mu$) and the Froude number ($Fr = V^2 \phi / g$) are the most commonly chosen non-dimensional numbers used in this area of research. The choice of any combination of the above-mentioned groups is arbitrary and, in the present work *We*, *Oh*, *Bo* and δ will be used, to try to separate the effects of the kinetic energy (ρV^2) and the liquid viscosity (μ).

When additional features are considered, like for example the surface roughness, the impact angle and the impact frequency, other non-dimensional numbers must be considered. Hence, the non-dimensional roughness R_{nd} ($R_{nd} = R_a/\phi$) and the non-dimensional impact frequency f_{nd} ($f_{nd} = f/f^*$, where f^* is, for example, equal to V/ϕ) can be taken into account. It is clear that R_{nd} becomes more important as the liquid film becomes thinner and the non-dimensional frequency has a threshold value above which interactions between successive splashes may take place.

Hereinafter, the term *splash* will be used to indicate the formation of secondary drops (droplets) after the impact of the impinging drop (the phenomenon shown in Fig. 1) and the term *deposition* will indicate an impact without production of secondary droplets. The drop deformation and splashing characteristics after impact on a dry solid wall depend on the drop velocity and the surface roughness (Worthington 1876; Engel 1967; Stow and Hadfield 1981). The critical velocity of the drop required to produce a splash increases with a decrease

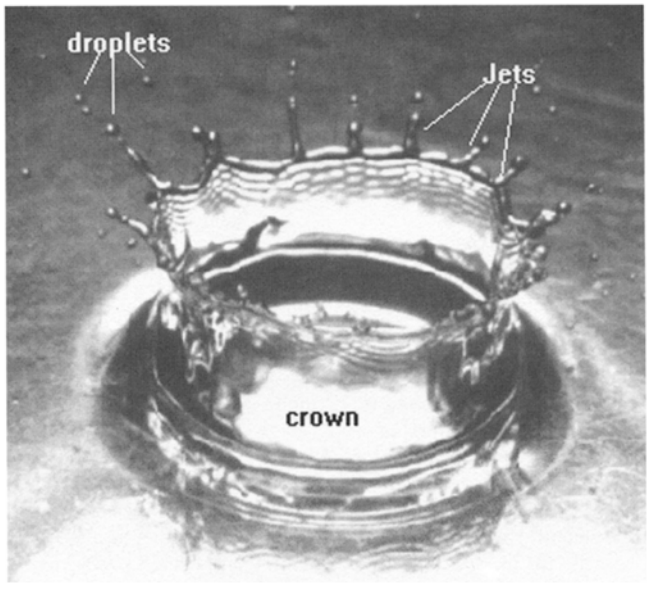

Fig. 1. The splash of a drop (scheme)

of surface roughness. For a dry surface, Stow and Hadfield (1981) found a correlation for the splashing/deposition limit which can be rewritten in terms of *Oh* and *We* as: $Oh^{-0.37}\ We = K_L'$; the correlation states that splash occurs when the drop Weber number and Ohnesorge number attain values such that the group $Oh^{-0.37}\ We$ is greater than K_L'. The threshold K_L' was found to depend on the surface roughness. Mundo et al. (1995) investigated the deposition/splashing limit using Reynolds and Ohnesorge numbers for impacts on a solid, dry surface. Very small drop diameters ($\phi < 150$ μm) were used. The limit found (again rewritten in terms of *We* and *Oh*) was: $Oh^{-0.40}\ We = 6.58 \times 10^2$ with no difference for the two values of roughness used ($R_{nd} = 0.03$ and $R_{nd} = 0.86$). The scaling behaviour was very similar to that proposed by Stow and Hadfield (1981) and in Fig. 2 the values of the splashing/deposition limit $K_L = (Oh^{-0.40}\ We)_L$ are plotted versus the nondimensional roughness, showing that the results from the different authors above mentioned are not inconsistent. The limit K_L decreases by increasing the nondimensional roughness reaching an asymptotic value for large values of R_{nd}. The fact that K_L increases sharply as the surface becomes smoother means that for very smooth surfaces the energy required for producing splash must become very high, a result already observed by Worthington (1876).

The splashing was found to be almost independent on the impact angle α (Mundo et al. 1995) in the range: $35° < \alpha < 87°$ (α is the angle between the drop trajectory and the wall) and the velocity component normal to the wall was used to evaluate *We* (or *Re*). For small impact angles ($\alpha < 10°$) Podvysotski and Shraiber (1993) found a complex empirical correlation for the splashing/deposition limit using a coalescence parameter Φ defined as the ratio between the mass of the liquid sticking to the wall and the liquid impinging on the wall; they showed that the coalescence increases with the increase of the collision angle, it is a non-monotonic function of viscosity, and strongly decreases with a decrease of roughness.

Stow and Stainer (1977) presented a large amount of experimental data about number and size of secondary droplets under different conditions of drop velocity and size, liquid surface tension and surface roughness. Plotting their results versus the number $K = Oh^{-0.4}\ We$, it is possible to observe a strict linear dependence of the number of secondary droplets on K when only data with $R_{nd} = 0.006$ (estimation of Stow and Hadfield 1981) are accounted for. In the limit for $N \to 0$ (N is the number of secondary droplets) of the linear fitting, $K = 1270$ is obtained, which can be considered an estimation of the splashing/deposition limit; this result is consistent to those shown in Fig. 2.

Splashing on a liquid surface was studied by many authors but most of the works treated the so called deep splash (i.e. when $\delta \gg 1$) whereas the study about splashing on thin liquid film (δ less than 1) are very few. A qualitative work of Gregory et al. (1959) showed that the number of secondary droplets decreases as the film thickness increases. The result was confirmed by Hobbs and Osheroff (1967); they also found that the height of the ejected jets (which are responsible of the droplet formation) decreases increasing the film thickness. Macklin and Metaxas (1976) found that a larger Weber number produces a thinner corona and an increase of the liquid volume in the corona. Following the theoretical approach of Engel (1966), they claimed that only about 5% of the impinging drop kinetic energy is carried away by the secondary droplets. They defined the splash as *deep* when the bottom of the target liquid container does not affect the splash and gave a limit for *shallow* ($\delta < 2$) and for *deep* splash ($\delta > 5$). They also found that the total volume of secondary droplets may reach (with high impact energy) 2 to 4 times the volume of the impinging drop.

Stow the Stainer (1977) investigated with some detail also the shallow splash regime. From their results a peculiarity can be inferred: surface roughness has an effect also when the surface is wet, in fact Fig. 3 shows that the number of secondary droplets is different for two values of the surface roughness, also in presence of a liquid film, and the influence becomes striking when the liquid film thickness becomes comparable to the roughness. The decrease of the number of secondary droplets with an increase of film thickness agrees qualitatively with the above mentioned observations of Gregory et al. (1959) and Hobbs and Osheroff (1967).

Walzel (1980) investigated the splashing/deposition limit with different mixtures of water and glycerol. The analysis was performed with a glass surface covered by a thin film ($\delta = 0.1$).

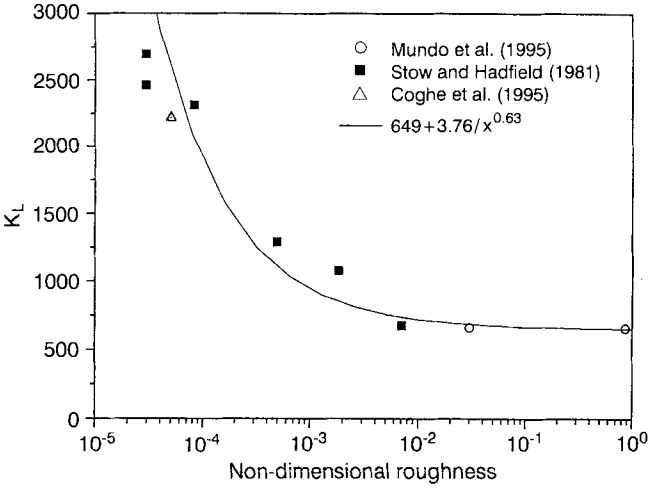

Fig. 2. Splashing/deposition limit (K_L) vs. nondimensional surface roughness for a drop impacting on a dry wall

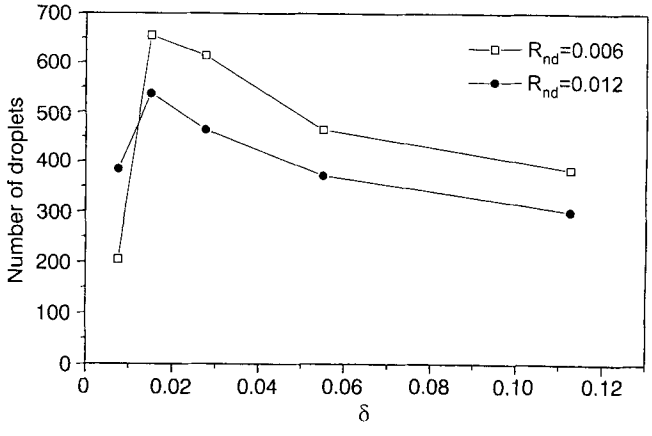

Fig. 3. Number of secondary drops vs film thickness for two nondimensional surface roughness (Stow and Stainer 1977; nondimensional roughness estimated from reported data)

The correlation for the splashing/deposition limit, again expressed in terms of Oh and We, can be written as: $Oh^{-0.4}\,We = 2.50 \times 10^3$. Again the group $K = Oh^{-0.4}\,We$ seems to play the main role in defining the splash threshold although Walzel (1980) results for dry surface led to the following correlation: $Oh^{-0.7}\,We = 7.9 \times 10^{10}$ which is in contrast to the previously mentioned results from other authors (the nondimensional roughness was surely very small and the small size of the impact disc, relatively to the drop diameter, may have had some influence due to edge effects on capillary flow).

Yarin and Weiss (1995) analysed theoretically and experimentally the general problem of the impact of a train of drops over an initially dry surface: they considered the impact frequency f and determined experimentally the splashing threshold to be $Ca\,\lambda^{3/4} = 17$, where $Ca = \mu V/\sigma$ is the capillary number and $\lambda = (\mu/\rho f)^{1/2}\sigma\rho/\mu^2$ is the viscosity length. Writing this correlation with the expression for a drop generator frequency $f = 3/2V/\phi\,(D/\phi)^2$, (where D is the nozzle diameter), and taking for the ratio D/ϕ the value 0.5 (which is an acceptable estimation from the data presented in the paper), the relation $We\,Oh^{-0.4} = 2.4 \times 10^3$ is found, again showing a scaling behaviour common to the previous mentioned works. The average film thickness was estimated by the authors to be between 20 and 50 μm (and $\delta \approx 0.17$). The theory proposed is based on the appearance of a kinematic discontinuity: assuming an initial form of the velocity distribution in the liquid film, they were able to describe the evolution of the discontinuity wave (the crown) and the motion law of the crown radius was found to take the form $(R_c/\phi) \div \tau^{1/2}$, where τ is the nondimensional time ($\tau = t\phi/V$).

The literature survey above reported suggests that the shallow splash regime can be subdivided into two sub-regimes, defined by the relative values of nondimensional film thickness and nondimensional surface roughness: (a) *thin* liquid film regime, where $\delta \gg R_{nd}$ and the surface morphology is not expected to influence significantly the splash (although some influence cannot be excluded); (b) *very thin* liquid film regime, where δ is comparable to R_{nd}, and strong influence of the surface morphology is expected.

3 Experimental set-up

The experimental set-up is shown in Fig. 4. Needles of different size produce pendant drops with diameters between 2 and 5.5 mm. The needles height (measured from the impact liquid surface) ranges between 0.05 and 2 m and a maximum terminal velocity of 6.5 m/s is obtained by producing a pressure pulse at the needle location which detaches the drop. The falling drop crosses two parallel laser beams, located close to the impact surface and imaged onto two photodiodes, and its flying time is measured by the delay between the sharp variation of the photodiode signal outputs, thus the drop velocity is obtained once the beams distance is known. The impact velocity measurement has an accuracy of about 5% depending primarily on the estimation of the distance between laser beams. The liquid film was generated by submerging an aluminium disk (0.1 m diameter, average roughness $R_a = 0.14$ μm) into a small tank. The vertical position of the disk could be varied with a precision of 10 μm. The liquid film thickness was measured using the following procedure: a pin was stuck on

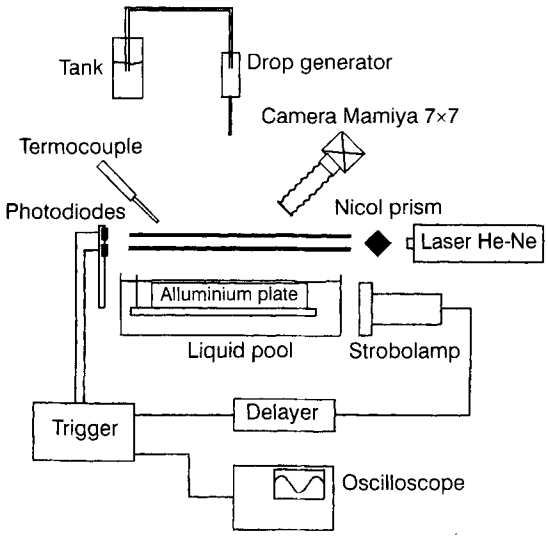

Fig. 4. The experimental set-up

the aluminium disk side and the distance of the pin tip from the disk upper surface was measured with an accuracy of 10 μm; the disk and the pin tip were completely submerged. Then a He–Ne laser beam was directed onto the liquid surface at the location where the pin tip will touch the liquid–air interface when lifted and its reflection was imaged onto a screen after magnification.

The disk (and the pin) was lifted up and the arrival of the pin tip at the liquid-air interface was detected by observing a change of uniformity in the beam image on the screen; the film thickness was then considered equal to the previously measured distance of the pin tip from the disk surface, and the wanted film thickness could then be obtained by furthermore lifting the disk. To limit the effect of the capillary meniscus, a very sharp and thin (<0.2 mm) pin was used. The overall accuracy of the procedure was estimated to be better than 30 μm.

The uniformity of the film thickness is controlled by the parallelism between the upper aluminium disk surface and the free liquid surface; in the first part of the experiment a high precision level was used, which allowed a nominal accuracy of the thickness uniformity to within 10 μm over the entire 0.1 m diameter of the disk. In the last part, a triangulation system based on the reciprocal positions of 3 pins was used, with comparable accuracy. To avoid large errors and for the strong instability of thinner films, a film thickness larger than 250 μm was used.

The splash was observed and recorded by a still-photo camera using two different techniques. For the first technique, the pictures were obtained by the illumination of a lamp whose flash duration was 10 μs. The lamp was controlled through a delay circuit triggered by the obscuration of a laser beam (detected by a photodiode) caused by the passage of the falling drop. By varying the delay between the trigger and the flash, the entire process could be recorded (Fig. 5). Thus, pictures of splash at different times and with different We, Oh, δ numbers were obtained, from which the number of jets on the crown, the formation of secondary droplets, the crown dimensions at

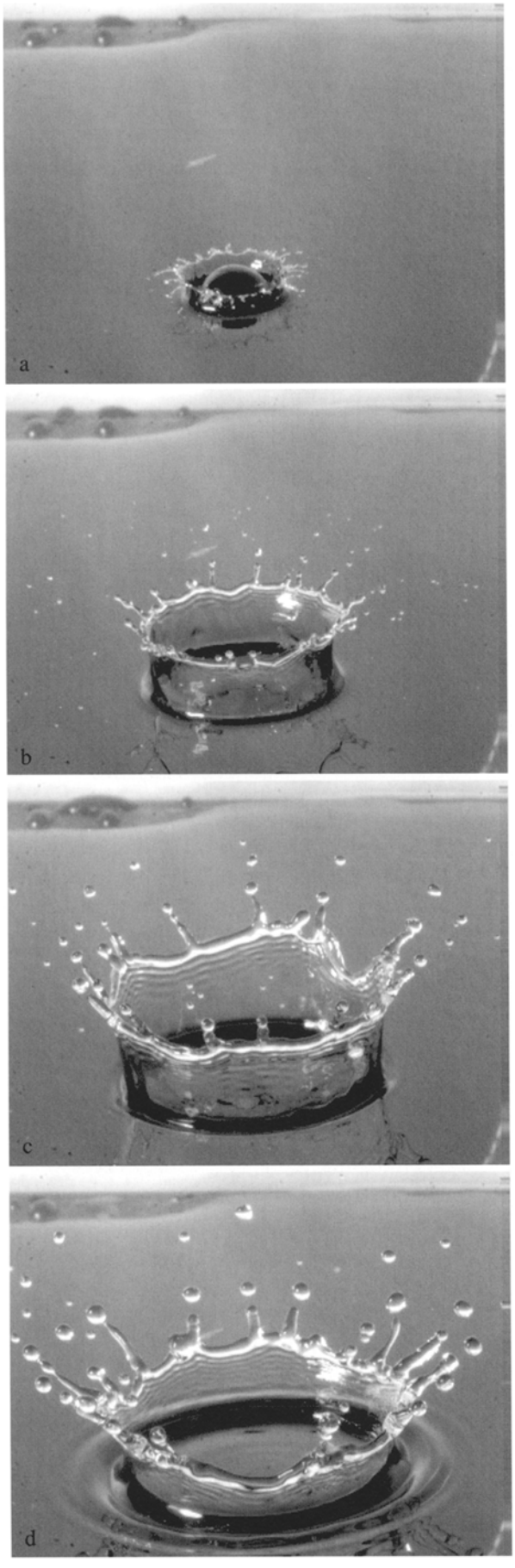

a given time after the impact can be evaluated. The second technique was used previously by Allen (1988): a light sheet obtained by expanding a laser beam through a cylindrical lens and a long focal spherical lens (to decrease the light sheet thickness) was directed toward the film in such a way that the trajectory of the falling droplets was encompassed by the sheet. The camera was kept open long enough to allow some drops to fall upon the film. In the pictures, the existence of secondary drops could be consistently observed over several impacts by the luminous traces of their trajectories (Fig. 6) and the threshold region between the splashing regime and the deposition regime can be defined. This technique has the advantage of allowing analysis of droplet kinematics (Allen 1988).

The drop diameter was measured for every needle scanning the picture shot immediately prior to impingement: by comparison to an object of known size, an accuracy better than 4% was obtained. To span a wide range of Ohnesorge number, water-glycerine mixtures were used, and the drop generator was positioned at different distances from the liquid layer to vary the Weber number. The liquid viscosity was measured with a Ubbelohde viscometer and the liquid temperature was monitored by means of a thermocouple. The accuracy on the viscosity measurement is about 1%. The surface tension and density of the used mixtures change very smoothly with the glycerol percentage and hence the available table values were used. Finally, the Weber number is defined within an accuracy of 15% and the Ohnesorge number accuracy is within 5%. The nondimensional film thickness (δ) is measured with an accuracy of 16% in the worst case (250 μm film thickness).

Following the simplified analysis of Macklin and Metaxas (1976), the ratio between the gravitational potential energy and the potential surface energy relative to the crown can be written as

$$\frac{U_g}{U_s} = \frac{g\rho h R_c}{\sigma} \frac{(h+H)}{4(h+2H)}$$

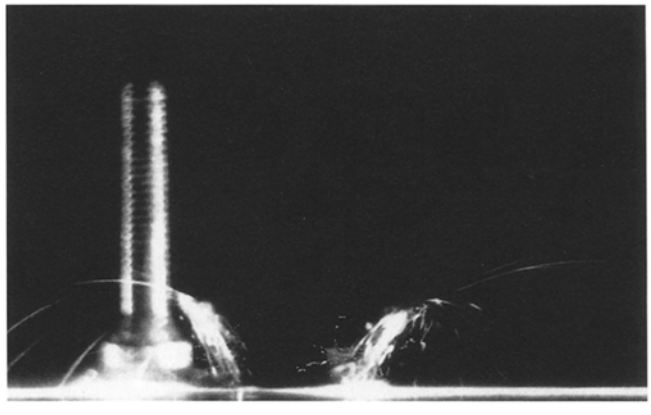

Fig. 6. Example of the laser sheet technique for splash detection. The droplet trajectories can be easily observed

Fig. 5a–d. The splash evolution (pictures of different events at different times after drop impact; $\delta = 0.5$, $Oh = 0.0022$). **a** $t = 0.4$ ms; **b** $t = 2.4$ ms; **c** $t = 6.4$ ms; **d** $t = 12.4$ ms

where H is the crown height and R_c the crown radius. By introducing the Bond number $Bo = \rho g h^2/\sigma$ and the nondimensional crown radius $R_{c,nd} = R_c/\phi$, the above mentioned ratio becomes equal to: $Bo\, R_{c,nd}/(8\delta)$ (when $H \gg h$). This nondimensional group can be taken as an estimation of the relative importance of the gravitation when compared to surface effects. In the present experiment, $0.12 < Bo/\delta < 1.2$ and $R_{c,nd} < 5$ approximately, so that the ratio U_g/U_s may range approximately between 0.075 and 0.75 (the greater value attained for $\delta = 1$ and $R_{c,nd} = 5$). That means that gravitation may play some role only for the largest value of the film thickness and in the late stage of the crown evolution (when R_c is large).

4
Results

A preliminary experiment was performed using pure water, to test the experimental set-up while gaining some information about the main features of the thin film splash phenomenon; in that case the drop diameter was 5.1 mm. Although this preliminary experiment was not performed in a methodical way, some of the results obtained are significant for the following discussion and they will be included. Subsequently, a systematic investigation about the splashing/deposition threshold was carried out in a wide range of experimental conditions: $2 \times 10^2 < We < 1.6 \times 10^3$, $2.2 \times 10^{-3} < Oh < 0.141$, $8 \times 10^{-2} < \delta < 1.2$, and $R_{nd} \cong 5 \times 10^{-5}$. In practice, only one nominal diameter for the impacting drop was used (ϕ was actually varying between 3.07 ± 0.07 mm for high viscosity, and 3.51 ± 0.06 mm for low viscosity). Pure water and four water glycerol mixtures were used, obtaining five nominal Ohnesorge number conditions (see Table 1). For each condition, six to ten different values of the nondimensional film thickness were analysed, and, for every thickness, the Weber number was changed by varying the height of the drop generator. Moreover, for sake of completeness, the splashing/deposition limit was investigated, for the above mentioned values of Ohnesorge number, also for dry surface ($\delta = 0$). Besides the quantitative results, a certain amount of information about the splash morphology and evolution was obtained through a careful observation of the still photographs.

4.1
Splash morphology

The evolution of the splash can be conveniently subdivided into four phases, whose characteristics can be observed through the pictures of Fig. 5: 1) crown formation and jetting (Fig. 5a), 2) rim instability and jet formation (Fig. 5b), 3) break-up of the jets and formation of secondary droplets (Fig. 5c), 4) crown collapsing period (Fig. 5d).

Table 1. Experimental conditions, nominal Onhesorge number is reported

Water	Glycerine 50% in water	Glycerine 65% in water	Glycerine 75% in water	Glycerine 81% in water
$Oh = 2.2$E-3	$Oh = 10.6$E-3	$Oh = 31.6$E-3	$Oh = 70.7$E-3	$Oh = 141$E-3

After the impact of a millimetric drop on a dry surface, a shock wave propagates into the drop till its apex; when the shock wave reaches the contact point between the splattering drop and the solid surface, an expanding wave is generated and a liquid flow is ejected from the drop border spreading along the surface and producing the so-called jetting flow (Field et al. 1985). From this jetting flow a lamella is formed and starts to propagate as a crown. Jetting flow appears to take place also for splash on thin film with a low liquid viscosity and, already in this phase, secondary droplets are detaching from the jetting flow.

However, with high viscosity liquid, secondary droplets were observed to detach only after full development of the crown. In this case the droplets may begin to detach from jets even during the crown collapsing period (Fig. 7). Thus, the viscosity appears to play an important role in defining the splash morphology and consequently the dynamic characteristics (size and velocity) of the secondary droplets. In the following, we shall consider two kinds of splash: a) the *prompt* splash, which takes place in the low Ohnesorge number regime, characterised by secondary atomisation already in the jetting phase; b) the *late* splash, in the high Ohnesorge number regime, when secondary atomisation takes place only from the jets protruded from the fully developed crown.

When crown is formed, it begins to increase in diameter and height. Along the crown two families of perturbation waves are visible: longitudinal waves and azimuthal waves (see Fig. 1). The longitudinal waves propagate vertically in the liquid sheet forming the crown and the azimuthal waves are visible in the form of periodical swallowing along the cylinder. Also a thicker rim is visible at the top of the crown and the azimuthal waves appear to be in correspondence of the roots of the jets. The motion of liquid inside the rim causes the formation of cusps and a simple explanation of the phenomenon is given by Yarin and Weiss (1995); however, a complete theory about the relation between the crown perturbations and the raising of jets has not yet been developed. The jets have low Reynolds number and they break-up through a Rayleigh process,

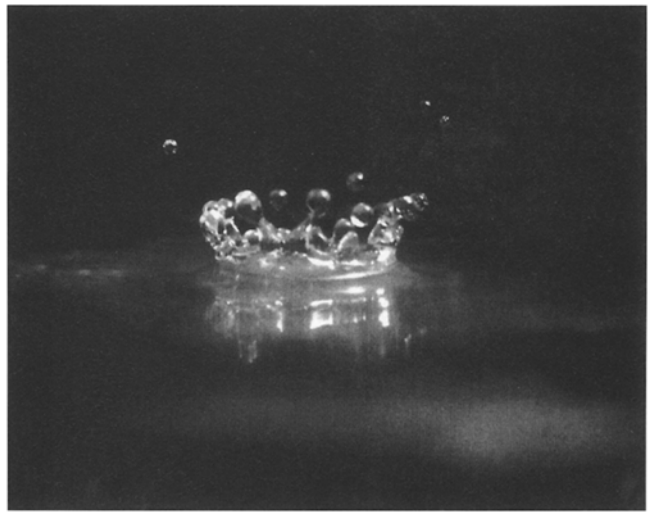

Fig. 7. Splash of a high viscosity drop (glicerine-water mixture 65%)

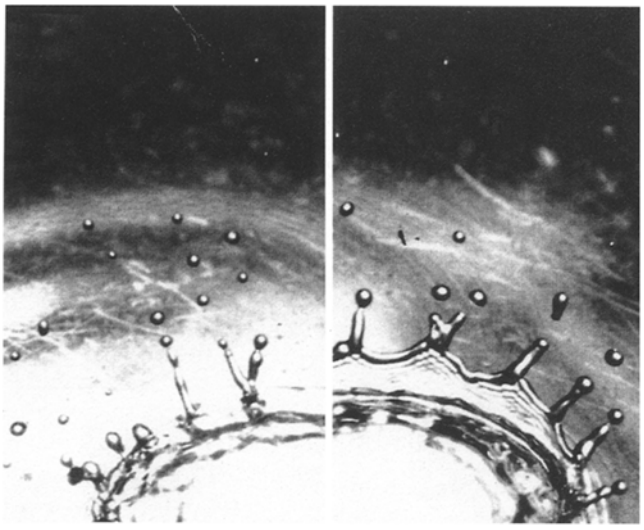

Fig. 8. Multi-branches jets on the crown

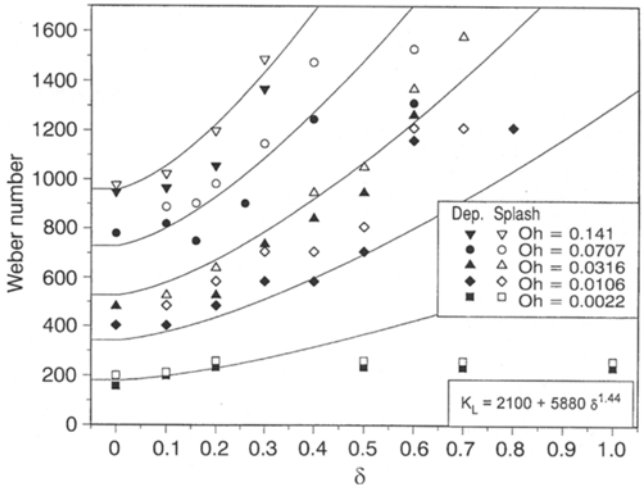

Fig. 9. Critical Weber number vs. film thickness for different values of Ohnesorge number

producing secondary droplets, as shown in Fig. 1 and Fig. 5c: from the pictures primary and satellite drops are clearly visible. It is also interesting to notice that some jets show peculiar characteristics like multiple branches, which may be due to coalescence of different jets at the initial stage (Fig. 8). The crown continues to grow during all the late splash phases and finally collapses. During the crown collapse, some bigger droplets are formed by the survived jets (Fig. 5d). No rim break-up (as observed by Mundo et al. 1995) was detected even with the maximum drop impact velocity allowed by the present experimental set-up.

4.2
The splashing/deposition limit

The splashing/deposition limit was investigated by analysing a large number of pictures, under conditions that spanned a quite wide range of Oh (see Table 1). Because of the high non-linearities involved in the splashing phenomenon and the experimental uncertainty above mentioned, it was not possible to observe a unique value of the critical Weber number for every pair of value of Oh and δ. Near the critical Weber number, nominally identical experimental conditions can give splash or deposition, so a minimum Weber number We_d, where no secondary droplets were ever observed and a maximum Weber number, We_s, where splash clearly occurred, were considered.

The difference $We_s - We_d$ for given values of δ and Oh was however found to be lower than $0.1 We_d$, i.e. less than the accuracy on evaluating Weber number itself. Figure 9 shows the values of the critical Weber number (open symbols for We_s, solid symbols for We_d) versus the nondimensional film thickness for different values of Oh; for a given Oh and a given δ splash certainly occurs when $We > We_s$ and deposition certainly occours when $We < We_d$.

For each value of Oh, the critical We (which can be defined as the average between We_d and We_s) increases with the increase of film thickness, i.e. increased thickness inhibits splashing. A decrease of the Ohnesorge number decreases the splashing threshold, which is an expected consequence of the viscosity damping of those perturbations which are likely to be responsible of jet formation and break-up. The values of We_d and We_s are reported in Table 2.

It is interesting to observe that the data relative to pure water (the lowest viscosity, $Oh = 0.0022$) does not show the same trend of all the others, in fact it seems that a sort of saturation exists when the film thickness increases. This fact is probably connected to the jetting flow which produces droplets since the very beginning of the splash and it is inhibited only when viscosity is higher. It appears as if the droplet production by prompt splash would need less energy (low We) to take place (it should be noticed that droplets produced at this stage are smaller then those produced by late splash).

From previous works, there is evidence that the splashing/deposition limit for impact over a wet solid surface (in the limit of a liquid film not thicker than the drop diameter) may be defined in terms of the nondimensional number $K = Oh^{-0.4} We$ and a general form of a possible correlation may be the following:

$$K_L = (Oh^{-0.4}\, We)_L = f(\delta, R_{nd}) \qquad (1)$$

The function $f(\delta, R_{nd})$ should satisfy some conditions based on physical considerations and available experimental data: a) for $\delta \to 0$ the function $f(0, R_{nd})$ should correlate the available experimental results for splash on dry surface (Stow and Hadfield 1981; Mundo et al. 1995, present results); b) for $\delta \gg R_{nd}$ the influence of the roughness should become neglectful. The experimental results for $\delta = 0$ can be correlated through the following equation: $f(0, R_{nd}) = g(R_{nd}) = 649 + 3.76/(R_{nd})^{0.63}$ and Fig. 2 shows the comparison with the available experimental data. In the present experiment the nondimensional roughness was about 5×10^{-5}, and it was kept constant; the experimental results with $\delta \geq 0.1$ where used to obtain an empirical correlation in the form $y(\delta) = A + B\delta^{\gamma}$ (which is the simplest form that correlates the data with acceptable consistency, and it should be understood as

Table 2. We_d and We_s for the different experimental conditions analysed

δ	Ohnesorge	Weber (deposition)	Weber (splash)
0	0.0022	157	200
0.1	0.0022	200	213
0.2	0.0022	234	259
0.5	0.0022	234	259
0.7	0.0022	234	259
1	0.0022	234	259
0	0.0106	404	
0.1	0.0106	404	485
0.2	0.0106	485	586
0.3	0.0106	586	707
0.4	0.0106	586	707
0.5	0.0106	707	808
0.6	0.0106	1161	1212
0.7	0.0106		1212
0.8	0.0106	1212	
0	0.0316	480	
0.1	0.0316		526
0.2	0.0316	526	639
0.3	0.0316	736	
0.4	0.0316	841	946
0.5	0.0316	946	1051
0.6	0.0316	1262	1367
0.7	0.0316		1577
0	0.0707	780	
0.1	0.0707	819	888
0.16	0.0707	749	902
0.2	0.0707		983
0.26	0.0707	902	
0.3	0.0707		1146
0.4	0.0707	1245	1474
0.6	0.0707	1310	1528
0	0.141	948	978
0.1	0.141	965	1024
0.2	0.141	1056	1198
0.3	0.141	1367	1486

Table 3. Values and accuracy of the parameters appearing into the empirical correlation (Eq. 2) of the experimental data about splashing/deposition limit

Parameter	A	B	γ
Value	2100	5880	1.44
Standard deviation	215	680	0.09

a possible form of the function: $f(\delta, R_{nd}=0.001)$). By applying a least square method the values of the parameters A, B and γ were found, and they are reported in Table 3 together with their standard deviations.

The correlation

$$K_L=(Oh^{-0.4}\,We)_L=2100+5880\delta^{1.44} \qquad (2)$$

also shown in Fig. 9 by solid lines, holds for $0.1<\delta<1$ and $Oh>7\times10^{-3}$ (actually, the correlation holds also for $Oh=2.2\times10^{-3}$ (pure water) but only for $\delta<0.2$ (see Fig. 9) with good accuracy, as reported in Table 3).

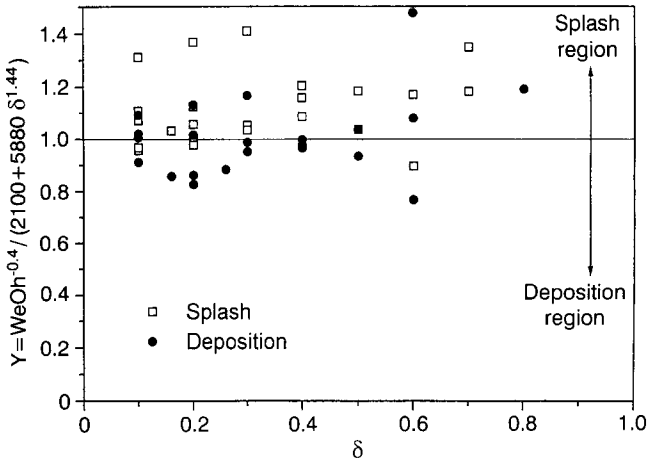

Fig. 10. The splashing parameter $Y=K_{L,\exp}/(2100+5880\delta^{1.44})$ vs. nondimensional film thickness

When the left side of Eq. (2) is greater than the right side, the splashing phenomenon with production of secondary droplets occurs.

Figure 10 shows the ratio between the experimental values of K_L and those evaluated through equation (2): $Y=K_{L,\exp}/(2100+5880\delta^{1.44})$. The horizontal line $Y=1$ defines a splash region ($Y>1$) and a deposition region ($Y<1$); points evaluated by using We_s (see above) are identified by open symbols to distinguish from those evaluated by using We_d (solid symbols). 83% of the points are comprised in the region: $0.8<Y<1.2$, and more than 80% of the experimental points are in the correct region, which gives an estimation of the accuracy of the correlation. A comparison between the other available results of Walzel (1980) ($K_L=2500$ with $\delta=0.1$) and Yarin and Weiss (1995) ($K_L=2400$ with $\delta\approx0.17$) and the proposed correlation ($K_{L,\mathrm{corr}}=2315$ for $\delta=0.1$ and $K_{L,\mathrm{corr}}=2560$ for $\delta=0.17$) should be considered satisfactory.

Extrapolation of Eq. (2) to $\delta\ll0.1$ should be considered arbitrary because, as above observed, the splashing limit for dry surface depends strongly on the roughness, and Eq. (2) does not contain R_{nd}. Figure 2 clarifies this statement and shows the consistency of the present result for dry surface with previous ones.

4.3 Number of jets, jet diameter and crown evolution after splashing

From the still photographs of the splash obtained in the above described experiments, the number of jets detaching from the crown (N_{jet}) was counted.

Figure 11 shows the N_{jet} probability density function (PDF) evaluated over all the available data from the present experiment; despite of the wide range of experimental conditions, the number of jets ranges in a relatively small interval (r.m.s. 2.45) around the mean value of about 11. No clear dependence of N_{jet} on We, Oh, δ and K was observed (except for the above mentioned difference in the PDF) and there are at least two possible reasons for this result: a) all the available pictures of

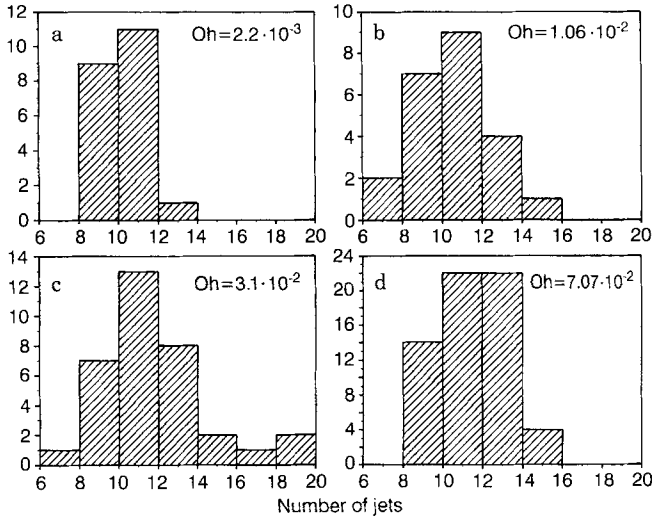

Fig. 11a–d. Distribution of the measured number of jets on the crown. **a** Pure water ($Oh = 0.0022$); **b–d** water-glycerine mixtures ($Oh > 0.01$)

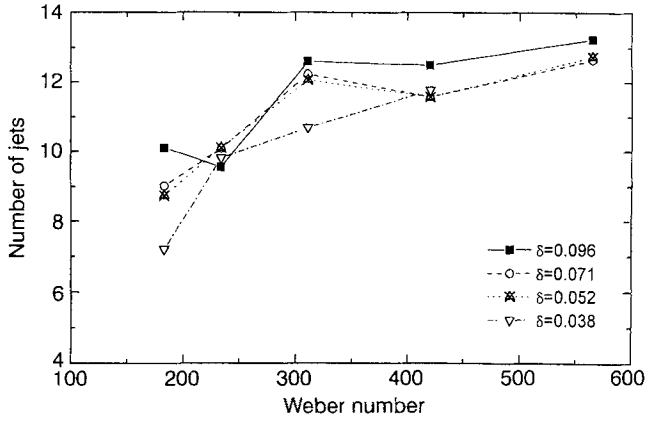

Fig. 12. Number of jets vs. Weber number (for pure water): $3000 < K < 8000$; $K_L \approx 2000$

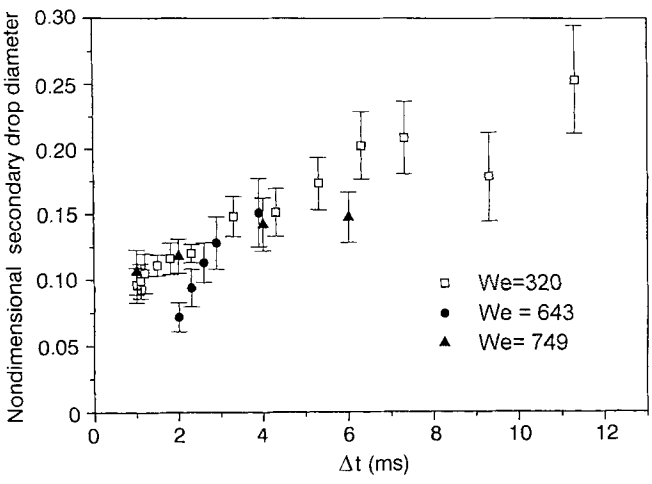

Fig. 13. Mean diameter (bars indicate the rms) of droplets detaching from the jets at different times. The measure of the diameter was performed only on detaching droplets (satellite droplets were not accounted for). The diameter was made dimensionless by the diameter of the primary drop. $Oh = 0.0022$

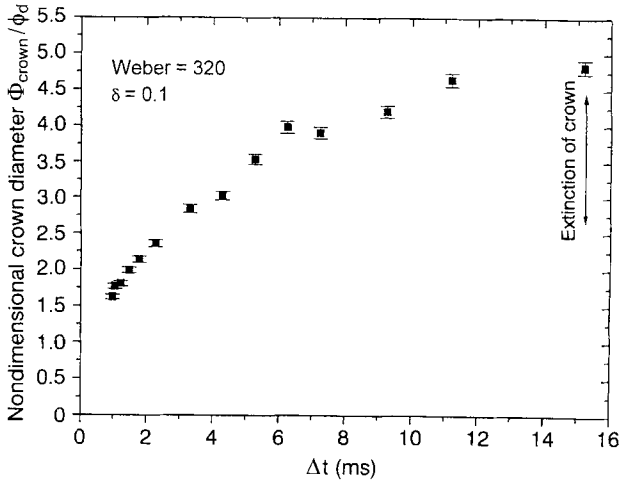

Fig. 14. Nondimensional crown diameter evolution (pure water)

the reported experiments were obtained in a relatively narrow region close to the splashing/deposition limit, but for conditions fully inside the splashing region the number of jets may depend on some parameters. In the preliminary experiment above mentioned a dependence of N_{jet} on Weber number was found (see Fig. 12). In that case pure water was used and K was ranging between 3000 and 8000 whereas the critical threshold (evaluated by Eq. (2), with δ lower than 0.1) was about 2000; b) only one nondimensional roughness was used, but the number of jets may depend on the surface morphology through its possible influence on the formation of perturbation on the crown; the preliminary experiment was performed with a solid surface having a higher roughness.

In the preliminary experiment (with pure water) the crown evolution was observed by taking pictures at different time after splash while maintaining the same experimental conditions. The diameter of the jets was observed to grow with time but a direct measure of their diameter from the pictures was not possible with an acceptable accuracy.

However, in Rayleigh break-up regime the detaching drop diameter is proportional to the jet diameter ($\phi_{drop} = 1.88\ \phi_{jet}$), thus measuring the size of only those droplets that are detaching from the jet (and excluding the satellite droplets which are usually smaller) quantitative information about the jet diameter can be obtained. Figure 13 shows the evolution of the average diameter of drops detaching at different times after impact. The increase with time has a possible explanation in the fact that when the crown begins to collapse, the rim, from which the jets protrude, increases in size by re-absorbing part of the crown, consequently the jet diameter increases.

Also the crown growth was observed and its diameter was measured (Fig. 14). The crown continues to grow during all the splash although the radial velocity decreases with time as already observed by Engel (1967). The Yarin and Weiss (1995) theoretical prediction of the crown size growth as a square root of time seems to be confirmed by the present data which are in agreement with measurements reported by Coghe and Cossali (1996).

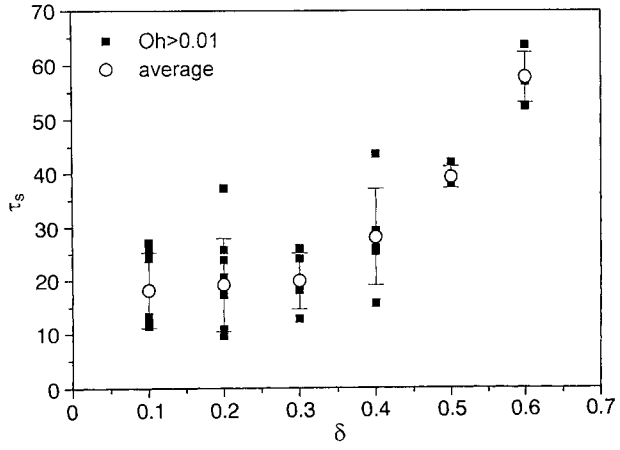

Fig. 15. Average value of τ_s vs. nondimensional film thickness (δ) for $Oh > 0.01$. Scattered data points correspond to different values of We; bars indicate the rms

4.4 Characteristic times

The ratio $\tau_0 = \phi/V$ has been commonly used as a time scaling factor in order to compare crown evolution in different experiments (Macklin and Metaxas 1980; Yarin and Weiss 1995). The present experimental set-up allowed to observe the splash at different times after drop impact, and to measure the time at which a given phenomenon takes place. The beginning of splash is difficult to define in an objective way but, in order to compare the duration of the phenomenon under different conditions, the nominal beginning of splash was defined as the time at which the droplets first detach from the jets. For all the conditions where splash was observed, the time of the splash beginning (t_s, the time of the first appearance of detaching droplets) was measured and non-dimensionalised by the time scale τ_0. For a given value of nondimensional film thickness, the data scattering around the mean value of $\tau_s = t_s/\tau_0$ was quite relevant. However, for $Oh > 0.01$, the average τ_s is dependent on δ as shown in Fig. 15, whereas it is independent of δ (average value: $\tau_{s,ave} = 3.7$) for pure water ($Oh = 0.0022$). The large difference between the experiments with water-glycerine mixtures and those with pure water is due to the fact that in the latter case *prompt* splash was observed. Those findings seem to support the idea that $\tau_0 = \phi/V$ is a correct way to scale the time, although allowances should be made for the effect of the film thickness.

5 Conclusions

The physical behaviour of a single drop impingement on a wetted, cold, solid surface was analysed and the following conclusions can be drawn.

A correlation for the splashing-deposition limit (under the condition: $\delta < 1$) was proposed in the form: $Oh^{-0.4}\, We = 2100 + 5880\delta^{1.44}$. This correlation shows an accuracy of about 10% around the experimental values and compares adequately with other available experimental results.

In the critical splashing/deposition region, the number of jets protruding from the crown was found to be independent of We, Oh and δ, whereas in an experiment under conditions well inside the splashing region ($Oh^{-0.4}\, We = 3000 \div 8000$ with $K_L = 2000$) with pure water and $\delta < 0.1$, an increase of the number of jets with Weber number was observed.

The jet diameter was found to increases with time, probably due to the increase of the rim produced by a partial re-absorbtion of the liquid forming the crown. The secondary droplet size distribution is therefore time dependent.

The diameter of the crown formed by the splash increases with time; for pure water a best fit in the form $R_c \div \tau^{1/2}$ was found, which seems to confirm the available theoretical predictions, but it is not conclusive due to the few data collected.

References

Allen RF (1988) The mechanics of splashing. J Colloid Interface Sci 124: 309

Baumeister KJ; Simon FF (1973) Leidenfrost temperature: its correlation for liquid metals, cryogens, hydrocarbons and water. Trans ASME Ser C J Heat Transfer: 95

Coghe A; Cossali GE; Marengo M (1995) A first study about Single Drop Impingement on thin liquid film in a low Laplace number range. Proc PARTEC'95, Nürnberg

Coghe A; Cossali GE (1996) Experimental analysis by laser extinction of the evolution of the liquid crown produced by the splash of a drop on a thin liquid film. 8th Int. Symp on Application of Laser Techniques to Fluid Mechanics, Lisbon

Edgerton HE; Killian JR (1954) Flash! Seeing the unseen by ultra high-speed photography. 2nd Edn. p. 106, Boston

Emmerson GS; Snoek CW (1978) The effect of pressure on the Leidenfrost point of discrete drops of water and Freon on a brass surface. Int J Heat Mass Transfer: 21

Engel OG (1967) Initial pressure, initial flow velocity and the time dependence of crater depth in fluid impact. J Appl Phys 38: 3935

Field JE; Lesser MB; Dear JP (1985) Studies of two-dimensional liquid-wedge impact and their relevance to liquid-drop impact problems. Proc R Soc London A 401: 225

Gregory PH; Guthrie EJ; Bunce ME (1959) Experiments on splash dispersal of fungs spores. J Gen Microbiol 20: 328

Hobbs PV; Osheroff T (1967) Splashing of drops on shallow liquid. Science 158: 1184

Levin Z (1970) Splashing of water drops: a study of hydrodynamics and charge separation: Ph.D. Thesis, Univ. of Washington

Levin Z; Hobbs PV (1971) Splashing of water drops on solid and wetted surfaces: hydrodynamics and charge separation. 269: 555

Macklin WC; Metaxas GJ (1976) Splashing of drops on liquid layers. J Appl Phys 47: 3963

Mundo Chr; Sommerfeld M; Tropea C (1995) Droplet–wall collisions: experimental studies of the deformation and breakup process. Int J Multiphase Flow 21: 151

Naber JD; Farrel PV (1993) Hydrodynamics of droplet impingement on a heated surface. SAE paper no 930919

Podvysotskii AM; Shraiber AA (1993) Experimental investigations of mass and momentum transfer in drop–wall interaction. Izv Mekh 2: 61

Stow CD; Hadfield MG (1981) An experimental investigation of fluid flow resulting from the impact of a water drop with an unyielding dry surface. Proc R Soc London 373: 419

Stow CD; Stainer RD (1977) The physical products of a splashing water drop. J Met Soc Japan 55: 518

Walzel P (1980) Zerteilgrenze beim Tropfenprall. Chem.-Ing.-Tech 52: 338

Worthington AM; Cole RS (1896) Impact with a liquid surface studied by the aid of instantaneous photography. Proc R Soc London 137–148

Yarin AL; Weiss DA (1995) Impact of drops on solid surfaces: self-similar capillary waves, and splashing as a new type of kinematic discontinuity. J Fluid Mech 283: 141